ISSN 0016-7029, Geochemistry International, 2020, Vol. 58, No. 11, pp. 1228–1238. © Pleiades Publishing, Ltd., 2020.
Russian Text © The Author(s), 2020, published in Geokhimiya, 2020, Vol. 65, No. 11, pp. 1080–1091.

Mass-Independent Sulfur Isotope Fractionation in the Photochemical SO_2 Processes under the UV Radiation of Different Wave Length

T. A. Velivetskaya[a], *, A. V. Ignatiev[a], and V. V. Yakovenko[a]

[a] *Far East Geological Institute, Far Eastern Branch, Russian Academy of Sciences, pr. 100-letiya Vladivostoku 159, Vladivostok, 690022, Russia*

**e-mail: velivetskaya@mail.ru*

Received February 9, 2020; revised April 8, 2020; accepted May 2, 2020

Abstract—A series of photochemical experiments with sulfur dioxide were carried out using a xenon lamp ($\lambda > 200$ nm), a low-pressure mercury lamp ($\lambda = 184.9$ and 253.7 nm), and an UP-213 laser system ($\lambda = 213$ nm) as light sources. Based on the isotope data obtained for elemental sulfur (the end product of SO_2 photolysis), we revealed specifics in correlations between $\delta^{34}S$, $\Delta^{33}S$, and $\Delta^{36}S$ values depending on the spectral characteristics of the incident radiation. Our studies showed that the Archean $\Delta^{33}S/\delta^{34}S$ and $\Delta^{36}S/\Delta^{33}S$ ratios could be reproduced in the SO_2 photolysis experiments by combining spectral composition of the radiation, the intensity of the spectral components, and the partial pressure of SO_2. The results of the experiments suggest that the UV radiation with wavelengths less than 200 nm was a determining factor in the production of sulfur isotopic anomalies in the Archean atmosphere.

Keywords: mass-independent fractionation, sulfur isotopes, early Earth atmosphere, Archean, photochemistry, sulfur dioxide

DOI: 10.1134/S0016702920110105

INTRODUCTION

Abstract—Mass-independent fractionation of sulfur isotopes (MIF-S) is a peculiar feature of sulfides and sulfates from Archean sedimentary rocks (>2.4 Ga). The MIF-S signal in the Archean rocks was discovered for the first time about twenty years ago (Farquhar et al., 2000). Farquhar et al. (2001) related the anomalous content of sulfur isotopes in the Archean sediments with photochemical reactions in the early Earth's atmosphere. Based on experimental studies, these authors suggested that the sulfur isotopic anomaly could be associated with photodissociation of sulfur dioxide (SO_2) in response to the ultraviolet (UV) radiation in the low-oxygen atmosphere. The end stable products of SO_2 photolysis are reduced (elemental sulfur S_8) and oxidized (H_2SO_4) sulfur species with positive and negative isotopic $\Delta^{33}S$ anomalies, respectively. During subsequent geochemical processes, the isotopic anomaly could be introduced in sedimentary sulfides and sulfates (Ono et al., 2003). According to the model calculations, the production of MIF-S in the atmosphere and transfer of this anomaly from atmosphere to the Earth's surface is possible if the content of free atmospheric oxygen is lower than 10^{-5} (the modern O_2 concentration in atmosphere) (Pavlov and Kasting, 2002). The presence of the MIF-S signal in the ancient sedimentary rocks is regarded as a convincing evidence for the absence of free atmospheric oxygen in the early atmosphere.

The mass-independent fractionation of sulfur isotopes during SO_2 photolysis was demonstrated in a series of experimental studies performed during last decade (Masterson et al., 2011; Whitehill and Ono, 2012; Ono et al., 2013; Endo et al., 2016; Endo et al., 2019; Ignatiev et al., 2019). Obtained experimental results demonstrate a spectral dependence of MIF effects. It was revealed that the mass-independent isotope fractionation during SO_2 photolysis varies in different spectral ranges. In particular, the UV-radiation yields a negative correlation between $\Delta^{33}S$ and $\Delta^{36}S$ isotopic anomalies in the photolysis products ($\Delta^{36}S/\Delta^{33}S \approx -1.90$) within wavelengths of 200–220 nm, and a positive correlation, within a range of 250–350 nm ($\Delta^{36}S/\Delta^{33}S \approx 0.64$) (Whitehill and Ono, 2012). The $\Delta^{36}S/\Delta^{33}S$ ratio in the SO_2 photolysis products may depend on the radiation intensities ratio in the ranges of 250–330 and 200–220 nm (Ignatiev et al., 2019). However, the relationships established between $\delta^{34}S$, $\Delta^{33}S$, and $\Delta^{36}S$ in the experiments are inconsistent with those observed in Archean rocks: $\Delta^{36}S \approx -0.9 \times \Delta^{33}S$ and $\Delta^{33}S \approx 0.9 \times \delta^{34}S$ (Ono, 2017). Therefore, the problems of sulfur sources and processes responsible for the production of MIF anomalies in the Archean rocks remain unresolved.

It should be noted that the above mentioned experimental studies were focused on the SO_2 photolysis within wavelengths >200 nm. It was suggested that the radiation in a shortwave region of the solar spectrum with wavelengths <200 nm was strongly suppressed in the Archean atmosphere owing to consumption by CH_4 and CO_2 gases in the troposphere. Therefore, isotope effects observed in Archean rocks are ascribed exclusively to SO_2 photodissociation in a wavelength range >200 nm (Lyons, 2007; Whitehill and Ono, 2012).

Based on experimentally determined relationships between mass-independent isotope fractionation during SO_2 photolysis and buffer gas pressure (Endo et al., 2019), the manner of MIF effects suggests either low pressure in an incipient atmosphere (<100 kPa) or the SO_2 photolysis reactions mainly in the upper atmosphere. Assuming that SO_2-assisted photochemical reactions were most intense in the stratosphere suggests an active role of shortwave (λ< 200 nm) solar UV in these processes.

According to the model concepts on the evolution of solar radiation fluxes (Ribas et al., 2010; Claire et al., 2012), the young sun emitted much more energy in a short-wave UV region than today's sun. Hence, the efficiency of atmospheric photochemical processes caused by intense UV solar flux was higher during Archean time than today. Hence, the SO_2 photolysis processes at wavelength λ < 200 nm played significant role in the production of MIF effects in the Archean atmosphere. In this relation, of great significance is to elucidate the isotope effects during SO_2 photolysis in a short-wave spectral range. For this purpose, photochemical experiments were carried out to determine the spectral dependence of MIF effects during SO_2 photolysis, varying relative radiation intensity at different wavelengths. Our experiments with different UV sources made it possible to establish relationships between $\delta^{34}S$, $\Delta^{33}S$, and $\Delta^{36}S$ in the photolysis products. Combining several radiation sources, we have demonstrated the dependence of $\Delta^{33}S/\delta^{34}S$ and $\Delta^{36}S/\Delta^{33}S$ on the spectral composition of radiation and spectral intensity. The results of experimental studies were analyzed to identify conditions responsible for the occurrence of Archean $\Delta^{33}S/\delta^{34}S$ and $\Delta^{36}S/\Delta^{33}S$ during SO_2 photolysis.

EXPERIMENTAL

Photochemical Experiments

The photochemical experiments on SO_2 photolysis were carried out using a system consisting of three main units: UV radiation source, flow reactor, and a gas inlet system. In our experiments, the following radiation sources were used: (1) xenon lamp (Xe lamp, 150 W) generating a continuous spectrum with wavelengths $\lambda \geq 200$ nm, (2) low-pressure mercury lamp (Hg lamp, 15 W) with discrete radiation at wavelength of 184.9 and 253.7 nm, (3) UP-213 laser system, New Wave Research (laser YAG:Nd, wavelength 213 nm). The Teflon reaction tube (inner diameter of 20 mm and length of 10 mm) has two flanges at the edge to mount window. The window is made up of magnesium fluoride (MgF_2), which is transparent in the UV and visible region of the spectrum. The reactor has ports for gas inlet and outlet. During experiments, the chamber was uninterruptedly blown off by pure SO_2 gas or gas mixture SO_2–He. The partial pressure of SO_2 (pSO_2) in a gas mixture varied from 2 to 1013 mbar.

We carried out several series of photochemical experiments aimed at estimating the variations of $\delta^{34}S$, $\Delta^{33}S$, and $\Delta^{36}S$ values in the SO_2 photolysis products depending on the spectral characteristics. The first experimental series was performed with Xe lamp for SO_2 radiation, while the second and third series were carried out using Hg lamp and UP-213 laser, respectively. Experimental parameters for these series are given in Table 1. In the subsequent experimental series, the total influence of Xe- and Hg-radiations on MIF effects during SO_2 photolysis (Xe–Hg experiments) was testified. For this purpose, SO_2 was simultaneously radiated by Xe and Hg lamps, which were respectively mounted before frontal and rear windows of chamber. In the Xe–Hg experiments, the intensity of Hg-radiation changed using slit located in front of the window. The size of the slit limited the flow of light energy of Hg lamp, whereas the radiation of Xe lamp remained unchangeable. In the final experimental series, we testified the variations of MIF effects during SO_2 photolysis under the influence of total radiation of UP-213 laser and Hg lamp (UP-213–Hg experiments). In these experiments, as in the Xe–Hg ones, the intensity of Hg-radiation varied, while parameters of laser radiation remained unchanged. The operation conditions of Xe–Hg and UP-213–Hg experiments are given in Table 2.

During photochemical experiments, the elemental sulfur and sulfur (VI) oxide precipitated on the inner walls of the reaction chamber. The elemental sulfur was extracted from the chamber by dissolution in hexane (C_6H_{14}) and subsequent evaporation of the latter. After solvent evaporation, all sulfur was fused in a homogenous mass. Obtained sample of elemental sulfur was used for isotopic analysis.

Sulfur Isotopic Analysis

The sulfur isotopic analysis of elemental sulfur samples obtained by photochemical reaction was analyzed using a local laser ablation fluorination (Ignatiev et al., 2018; Velivetskaya et al., 2019). The laser ablation of sulfur samples was carried out using a femtosecond laser complex (New Wave Research Division, Portland, OR, USA). The fluorination of laser ablation products was conducted in a flow nickel reactor at 350°C in the presence of bromine pentafluoride (BrF_5). The SF_6 pro-

Table 1. Experimental conditions with different radiation sources (Xe and Hg lamps, laser system UP-213) and results of isotope analyses in products (elemental sulfur) of SO_2 photolysis.

Experimental conditions		Isotope data								
pSO_2, mbar	SO_2 column density, molecule/cm^2	$\delta^{34}S$, ‰	1σ	$\Delta^{33}S$, ‰	1σ	$\Delta^{36}S$, ‰	1σ	N	$\Delta^{33}S/\delta^{34}S$	$\Delta^{36}S/\Delta^{33}S$
Xe lamp										
5	1.3E+17	39.0		3.83		−14.3		1	0.10	−3.7
12	3.2E+17	57.2	1.0	6.15	0.73	−15.1	0.1	2	0.11	−2.5
20	5.4E+17	92.6		7.56		−20.8		1	0.08	−2.7
50	1.3E+18	110.8		8.42		−27.0		″	0.08	−3.2
70	1.9E+18	108.1		8.15		−27.8		″	0.08	−3.4
73	2.0E+18	117.8		7.27		−26.7		″	0.06	−3.7
200	5.4E+18	107.7		6.61		−25.7		″	0.06	−3.9
300	8.1E+18	103.6		5.65		−23.1		″	0.05	−4.1
320	8.6E+18	105.3		5.11		−22.3		″	0.05	−4.4
333	9.0E+18	109.3		4.73		−23.2		″	0.04	−4.9
360	9.7E+18	100.4	4.6	5.03	0.03	−21.5	0.9	3	0.05	−4.3
417	1.1E+19	97.6		4.04		−20.9		1	0.04	−5.2
558	1.5E+19	83.4	0.1	3.30	0.10	−19.7	0.2	2	0.04	−6.0
630	1.7E+19	75.3	3.3	2.50	0.15	−16.6	0.3	2	0.03	−6.6
700	1.9E+19	73.6		3.34		−14.5		1	0.05	−4.3
1013	2.7E+19	55.7	3.3	1.92	0.29	−10.5	0.3	5	0.03	−5.5
Hg lamp										
2.1	5.6E+16	−325.4		556.05		549.1		1	−1.71	1.0
3.7	9.9E+16	−326.6		563.19		556.4		″	−1.72	1.0
12	3.2E+17	−328.2		566.31		553.4		″	−1.73	1.0
20	5.4E+17	−330.1		566.65		547.1		″	−1.72	1.0
25	6.7E+17	−327.5		563.92		548.6		″	−1.72	1.0
45	1.2E+18	−322.2		562.41		535.2		″	−1.75	1.0
50	1.3E+18	−316.8		557.63		525.1		″	−1.76	0.9
70	1.9E+18	−323.1		556.11		528.7		″	−1.72	1.0
83	2.2E+18	−319.8	0.8	549.20	1.38	521.1	2.0	4	−1.72	0.9
200	5.4E+18	−301.9		516.83		493.5		1	−1.71	1.0
1013	2.7E+19	−226.0	3.1	349.77	4.44	334.9	7.1	2	−1.55	1.0
UP-213										
70	1.9E+18	870.9	5.9	−26.6	0.9	−391.9	4.3	2	−0.03	14.7
1013	2.7E+19	626.9	25.1	−13.6	0.2	−276.0	19.4	2	−0.02	20.3

N—number of experiments, σ—standard deviation.

duced by fluorination was purified from other reaction products by cryogenic and chromatographic separation and then was introduced into ion source of the mass spectrometer (MAT 253, Thermo Scientific, Bremen, Germany). The sulfur isotope ratios in SF_6 was determined by simultaneous measurement of ion currents m/z 127 ($^{32}SF_5^+$), 128 ($^{33}SF_5^+$), 129 ($^{34}SF_5^+$) and 131 ($^{36}SF_5^+$). The results of isotopic analyses in samples are given relative to the initial SO_2 gas used in

Table 2. Conditions of Xe–Hg and UP-213–Hg experiments and results of isotope analyses in products (elemental sulfur) of SO_2 photolysis

Experimental conditions				Isotope data								
pSO_2, mbar	SO_2 column density, molecule/cm^2	% Xe lamp	% Hg lamp	$\delta^{34}S$, ‰	1σ	$\Delta^{33}S$, ‰	1σ	$\Delta^{36}S$, ‰	1σ	N	$\Delta^{33}S/\delta^{34}S$	$\Delta^{36}S/\Delta^{33}S$
Xe–Hg experiment												
1013	2.7E+19	100	100	–247.6		445.2		399.1		1	–1.8	0.9
″	″	″	35	–75.2		171.8		115.2		″	–2.3	0.7
″	″	″	15	–5.9		103.2		50.6		″	–17.6	0.5
″	″	″	5	45.5		44.3		–2.6		″	1.0	–0.1
170	4.6E+18	″	100	–140.7	1.4	219.7	2.0	189.6	1.6	3	–1.6	0.9
″	″	″	35	–44.1		123.5		74.1		1	–2.8	0.6
″	″	″	15	19.4		58.6		6.4		1	3.0	0.1
″	″	″	5	99.5	1.0	32.9	0.1	–12.0	0.3	2	0.3	–0.4
70	1.9E+18	″	10	76.0		75.1		23.6		1	1.0	0.3
″	″	″	5	106.7		37.6		–5.4		″	0.4	–0.1
″	″	″	2	124.2		18.5		–22.1		″	0.1	–1.2
UP-213–Hg experiment												
70	1.9E+18	100*	25	595	2.9	68.6	0.4	–248.9	2.3	2	0.1	–3.6
70	1.9E+18	″	55	261	1.8	199.3	1.5	–36.3	1.6	2	0.8	–0.2

N—number of experiments, σ—standard deviation, *—data on UP-213.

photochemical experiments. The isotope data are given in the generally accepted form: $\delta^X S = \left({}^X R_{sample} / {}^X R_{SO_2} - 1\right) \times 1000$, where ${}^X R = {}^X S/{}^{32} S$ (X = 33, 34, or 36) in sample (R_{sample}) and initial gas SO_2 (R_{SO_2}), respectively. The deviation from mass-independent isotope fractionation (isotope anomaly) is designated as Δ and can be written as follows:

$$\Delta^{33}S = \delta^{33}S - 1000\left[\left(1 + \frac{\delta^{34}S}{1000}\right)^{0.515} - 1\right],$$

$$\Delta^{36}S = \delta^{36}S - 1000\left[\left(1 + \frac{\delta^{34}S}{1000}\right)^{1.90} - 1\right].$$

The reproducibility of the results (1σ) in the replicate analyses of international standards IAEA-S-1 was 0.15‰, 0.02‰, and 0.3‰ for $\delta^{34}S$, $\Delta^{33}S$, and $\Delta^{36}S$, respectively.

RESULTS AND DISCUSSION

Mass-Independent Sulfur Isotope Fractionation in Experiments with Xe Lamp and Low-Pressure Hg Lamp

In the experimental series with Xe lamp, $\delta^{34}S$, $\Delta^{33}S$, and $\Delta^{36}S$ isotope effects shows a clear dependence on the SO_2 partial pressure (Table 1) with correlations $\Delta^{33}S = 0.06 \times \delta^{34}S$ and $\Delta^{36}S = -3.7 \times \Delta^{33}S$ (Fig. 1). These experimental dependences are similar to those established in analogous experiments with Xe lamp by Whitehill et al. (2012) ($\Delta^{33}S/\delta^{34}S = 0.15$ and $\Delta^{36}S/\Delta^{33}S = -1.9$) and Ono et al. (2013) ($\Delta^{33}S/\delta^{34}S = 0.08$ and $\Delta^{36}S/\Delta^{33}S = -4.6$). Note that our experiments with Xe lamp were not aimed at obtaining any new experimental facts, but served only as the basis for subsequent experiments and, respectively, assessment of isotope effects.

Results of experiments with Hg lamp are presented in Table 1. These experiments, as experiments with Xe lamp, demonstrated the dependence of sulfur isotope fractionation on pSO_2; the magnitude of isotope effects significantly decreased in the high pSO_2 region (Fig. 2). The difference in isotope data between experiments with Hg and Xe lamps is as follows. The isotope fractionation in experiments with Hg lamp is much higher than in experiments with Xe lamp (Figs. 1, 2). The $\delta^{34}S$ values are negative in experiments with Hg lamp, and positive in experiments with Xe lamp. Experiments with Hg and Xe lamps also yield opposite signs of $\Delta^{36}S$. Therefore, correlations $\Delta^{33}S = -1.72 \times \delta^{34}S$ and $\Delta^{36}S = 0.96\ \Delta^{33}S$ obtained in Hg experiments sharply differ from those in Xe experiments (Figs. 1, 2). Results of these experiments confirmed that sulfur isotope fractionation during SO_2 photolysis is determined by the spectral characteristics of radiation.

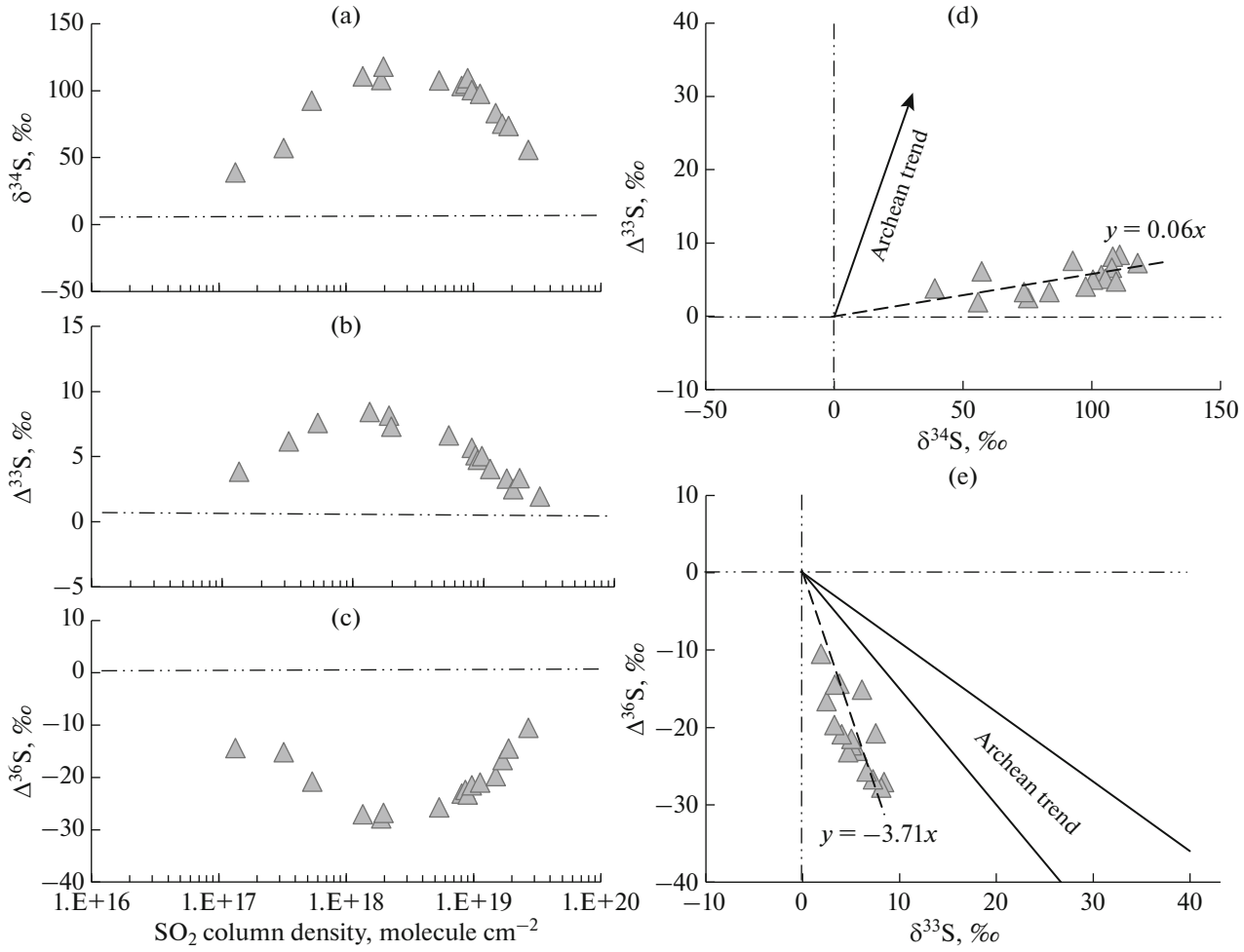

Fig 1. Results of photochemical experiments with Xe lamp. (a–c) variations of $\delta^{34}S$, $\Delta^{33}S$, and $\Delta^{36}S$ in the elemental sulfur (product of SO_2 photolysis) depending on density of SO_2 column in photochemical chamber. (d) correlation $\Delta^{33}S-\delta^{34}S$ and (e) $\Delta^{36}S-\Delta^{33}S$ in elemental sulfur. Dashed lines in Figs. 1d and 1e show experimental isotope trends. Solid line shows Archean trends.

A spectrum of low-pressure Hg lamp comprises two most intense resonance lines at wavelengths 253.7 and 184.9 nm, with more than 80% of the radiation being at the 253.7 nm line.

At the same time, precisely 184.9 nm radiation determines the character of isotope effects in Hg experiments. Since absorption by SO_2 molecules in the 185-nm region is almost two orders of magnitude higher than in the 254-nm region, the isotope effects could be mainly controlled by photochemical processes initiated by 185 nm radiation. This was verified in the additional experiments with Hg lamp, isolating $\lambda \approx 185$-nm radiation by optical filter. The filter was placed between Hg lamp and output window of photochemical chamber. The absence of 185 nm radiation changed isotope effects $\delta^{34}S = -23.3‰$, $\Delta^{33}S = 6.4‰$, and $\Delta^{36}S = 23.1‰$. These considerations showed that the isotope effects in experiments with Hg lamp are defined by 184.9 nm line.

A magnitude of MIF effects and slopes of isotope trends ($\Delta^{33}S/\delta^{34}S \approx -1.7$ and $\Delta^{36}S/\Delta^{33}S \approx 1.0$) observed in our Hg-experiments are well consistent with results of previous studies (Farquhar et al., 2001) obtained in similar experiments with Hg resonance lamp ($\Delta^{33}S/\delta^{34}S \approx -1.7$ and $\Delta^{36}S/\Delta^{33}S \approx 0.6$). Unlike previous studies (Farquhar et al., 2001), we testified the dependence of MIF effects on the SO_2 partial pressure within a wide range of pSO_2 values from 1013 to 5 mbar. Isotope data obtained in our experiments showed that SO_2 photolysis initiated by Hg radiation cannot produce isotope anomalies typical of Archean rocks. Experimentally established values of $\Delta^{33}S/\delta^{34}S \approx -1.7$ and $\Delta^{36}S/\Delta^{33}S \approx 1.0$ in the photolysis products sharply differ from those of Archean rocks ($\Delta^{33}S/\delta^{34}S \approx 0.9$ and $\Delta^{36}S/\Delta^{33}S \approx -1.0$).

It should be noted that Hg-experiments provide insight into the MIF effects during SO_2 photolysis in a

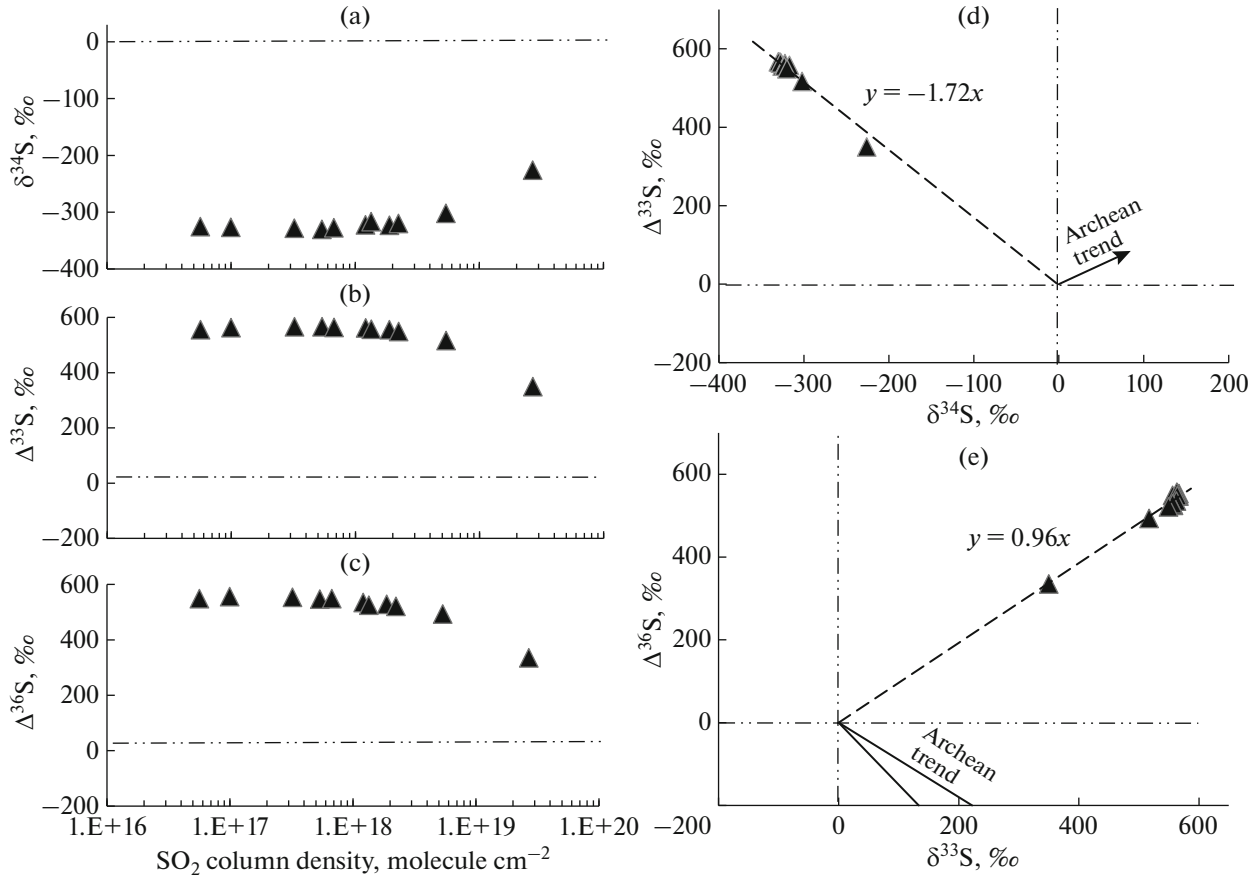

Fig. 2. Results of photochemical experiments with Hg lamp. (a–c) variations of $\delta^{34}S$, $\Delta^{33}S$, and $\Delta^{36}S$ in elemental sulfur (product of SO_2 photolysis) depending on density SO_2 column in photochemical chamber. (d) correlation $\Delta^{33}S-\delta^{34}S$ and (e) $\Delta^{36}S-\Delta^{33}S$ in elemental sulfur. Dashed line in Figs. 1d and 1e shows experimental isotope trends. Solid line shows Archean trends.

relatively narrow wavelength range. The possibilities of application of experimental results with a narrowband sources for explanation of MIF effects in Archean rocks was considered in (Lyons 2009; Claire et al., 2014). It was shown that a direct comparison of experimental results with Archean trends has no a physical meaning for experiments with a narrowband source (<1 nm), in particular, with a monochromatic light source, which could cause a selective excitation of one of sulfur isotopes during SO_2 photolysis. A selective excitation was caused by difference between energetic levels of vibrational states of molecules containing atoms of different isotopes. Therefore, radiation with a definite wavelength λ will be selectively absorbed by molecules of one isotope type, converting them into excited state, and does not interact with molecules of other isotope type. To cause a selective excitation, a shift between vibrational energy levels for different isotope molecules should be higher than the width of their energetic levels. SO_2 molecule has a structured electron-vibrational absorption spectrum (Manatt, Lane, 1993). Absorption spectra of isotopically substituted forms of $^{32}SO_2$, $^{33}SO_2$, $^{34}SO_2$, and $^{36}SO_2$ molecules show a slight difference in the position, width, and amplitude of peaks for different SO_2 isotopologs (Danielache et al., 2008; Endo et al., 2015). Difference in SO_2 isotopologs spectra is sufficient to provide the enrichment or depletion of SO_2 photolysis products in definite isotope, if radiation has a very narrow width of spectral band (<1 nm), for instance, laser radiation. Based on calculations, Claire et al. (2014) predicted that a shift of wavelength of ArF-excimer laser (193 nm) only for 0.5 nm (192.5 nm) will result in a change of a positive sign for negative for $\Delta^{33}S$ values in the SO_2 photolysis product. The photochemical laser separation of isotopes requires monochromatic and intense radiation. In this respect, the Hg gas-discharge lamp used in our Hg experiments, in spite of the narrow spectral range, is not a strictly monochromatic source. Resonance radiation of mercury lamp spans several wavelengths from different Hg isotopes; for instance, ultra-fine isotopic structure of 253.7 nm Hg resonance band contains several mutually overlapped bands within 5-nm region (Vyazovetskii and Vyazovetskii, 2013). Hence, MIF effects observed in

the Hg experiments were not caused by a monochromatic radiation; the use of Hg lamp is quite possible for study of conditions of production of MIF effects in Archean rocks.

The comparison of isotope data obtained in experiments with low-pressure Hg lamp (discrete radiation $\lambda = 184.9$ and 253.7 nm) with data obtained previously in experiments with high-pressure Hg lamp (continuous radiation spectrum) (Ignatiev et al., 2019) revealed no difference in isotope effects. Both for resonance and continuous radiation, the presence of 184.9 nm-band is responsible for the manifestation of isotope effects with $\Delta^{33}S/\delta^{34}S = -1.7$ and $\Delta^{36}S/\Delta^{33}S = 0.9$. Thus, if 184.9-nm band is present in a continuous radiation spectrum, the magnitude of isotope effects and values of $\Delta^{33}S/\delta^{34}S$ and $\Delta^{36}S/\Delta^{33}S$ should depend on the intensity of this band. The intensity of radiation affects the amount of formed photodissociation products and, hence, indirectly, the total isotope effect during SO_2 photolysis in the considered spectral range.

In the experimental series with two radiation sources, Xe lamp and low-pressure Hg lamp, we have analyzed variations of $\Delta^{33}S/\delta^{34}S$ and $\Delta^{36}S/\Delta^{33}S$ ratios at different modes of SO_2 radiation.

Mass-Independent Fractionation of Sulfur Isotopes in the Xe–Hg and UP-213–Hg Experiments

Results of Xe–Hg experiments are presented in Table 2 and shown in Figs. 3a, 3b. Three Xe–Hg experimental series were carried out at pSO_2 = (1013, 170, and 70) mbar. In each of these series, the intensity of Hg-radiation changed at constant Xe-radiation. Experimental tendencies established in the Xe–Hg experiments are as follows. With decrease of intensity of Hg radiation, the value of $\delta^{34}S$ changes from negative to positive values, while values of $\Delta^{36}S$, in contrast, from positive to negative ones, and the magnitude of $\Delta^{33}S$ anomaly decreased. Isotope data from three Xe–Hg experimental series for pSO_2 = (1013, 170, and 70) mbar define $\delta^{34}S$–$\Delta^{33}S$ and $\Delta^{33}S$–$\Delta^{36}S$ trends, which connect initial data of Xe- and Hg experiments (Figs. 3a, 3b). The values of $\Delta^{33}S/\delta^{34}S$ and $\Delta^{36}S/\Delta^{33}S$ varied from −1.8 to 0.1 and from 0.9 to −1.2, respectively.

Results of Xe–Hg experiments showed that variations of MIF effects and $\Delta^{33}S/\delta^{34}S$ and $\Delta^{36}S/\Delta^{33}S$ ratios are determined by a combination of spectral composition, intensity of spectral components, and partial pressure of gas components. It is expected that definite combination of these parameters will yield MIF effects comparable with Archean values of $\Delta^{33}S/\delta^{34}S \approx 0.9$ and $\Delta^{36}S/\Delta^{33}S \approx -0.9$. In our Xe–Hg experiments, we obtained relations close to Archean values $\Delta^{33}S/\delta^{34}S = 1.0$ and $\Delta^{36}S/\Delta^{33}S = -1.2$ at constant $pSO_2 = 70$ mbar and 10 and 2% decrease of light flow of Hg lamp, respectively (Figs. 3c, 3d). The experiments demonstrated that MIF anomalies in the Archean rocks can be explained with allowance for previously unaccounted photochemical SO_2 reactions with a short-wave radiation (<200 nm). The relations between intensities of spectral components from short-wave and longer wave regions should cause the total effect of isotope fractionation in SO_2 photolysis product in different spectral regions. The dependence of MIF effects on the intensity of spectral components was demonstrated in the UP-213-Hg experiments.

The UP-213–Hg experiments, unlike Xe–Hg experiments, were carried out with a laser source instead of Xe lamp, i.e., a continuous radiation with $\lambda > 200$ nm was replaced for a monochromatic radiation with wavelength $\lambda = 213$ nm. Results of these experiments are shown in Table 2. Our UP-213–Hg experiments established the dependence of $\Delta^{33}S/\delta^{34}S$ and $\Delta^{36}S/\Delta^{33}S$ on the Hg radiation intensity. The $\Delta^{33}S/\delta^{34}S$ and $\Delta^{36}S/\Delta^{33}S$ values lie along the corresponding straight lines, which connect the initial data of Hg-experiments with data of laser experiments (Figs. 4a, 4b) and are intersected with a region of Archean trends. Such a behavior of MIF effects represents a general tendency expressed in experiments with laser sources and Xe lamp. However, the value of $\delta^{34}S$ and $\Delta^{36}S$ isotope effects in experiments with laser radiation (213 nm) is almost an order of magnitude higher than those in experiments with a wide-band radiation (>200 nm).

At the same time, the results of the considered experiments revealed a common problem. Experimentally produced MIF effects are well consistent with Archean trends either for $\Delta^{33}S/\delta^{34}S$ or for $\Delta^{36}S/\Delta^{33}S$ ratios, not for both ratios simultaneously at a given combination of parameters in experiment. For instance, as mentioned above, combining radiation parameters in the Xe–Hg experiments ($pSO_2 \approx 70$ mbar and Hg lamp ≈10%) could yield a good agreement of $\Delta^{33}S/\delta^{34}S$ ratios with Archean values ($\Delta^{33}S/\delta^{34}S = 1.0$), but $\Delta^{36}S/\Delta^{33}S$ ratios fall beyond the region of Archean values (Figs. 3c, 3d). In contrast, if agreement is reached for $\Delta^{36}S/\Delta^{33}S$, it is not fulfilled for $\Delta^{33}S/\delta^{34}S$ (Figs. 3c, 3d). This fact hampers the determination of conditions of MIF effects production in the early atmosphere from experimental results.

Simultaneous coincidence of experimental $\Delta^{33}S/\delta^{34}S$ and $\Delta^{36}S/\Delta^{33}S$ values with Archean trends is obligatory condition for the identification of a source of MIF signal in the Archean rocks. Our experimental results can be used to simulate conditions when such coincidence becomes possible. Let's use the data obtained by Farquhar et al. (2001) in ArF excimer laser ($\lambda = 193$ nm) experiments. The following isotope data on elemental sulfur (product of photochemical reactions) were obtained: $\delta^{34}S = -42.0‰$, $\Delta^{33}S = 67.2‰$, $\Delta^{36}S = -48.4‰$ (Table 1, Farquhar et al., 2001). In Figs. 5a, 5b, these data were connected with data of our Xe–Hg

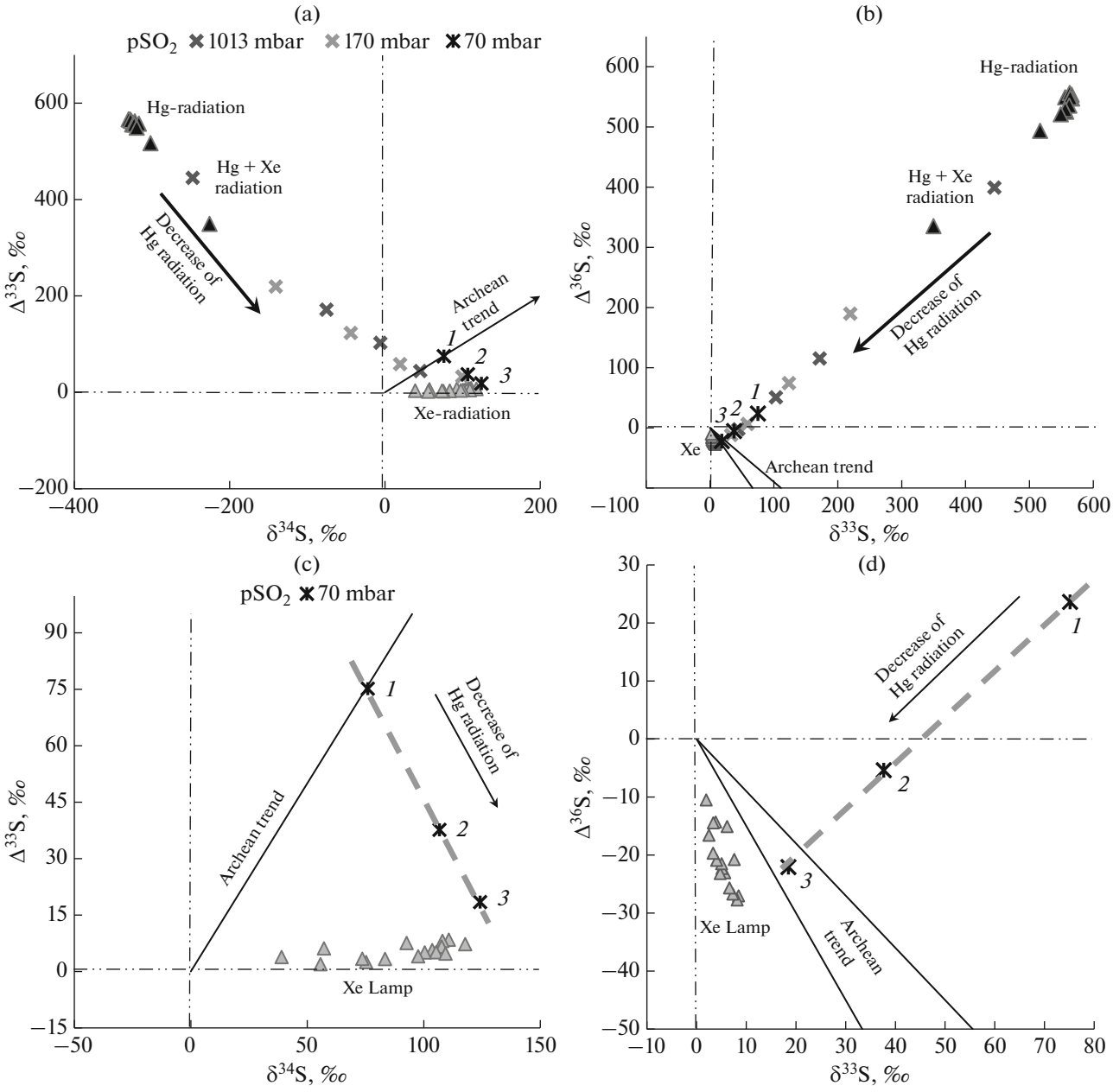

Fig. 3. Relations between $\Delta^{33}S$ and $\delta^{34}S$ (a) and between $\Delta^{33}S$ and $\Delta^{36}S$ (b) for elemental sulfur (product of SO_2 photolysis), obtained in experiments with a simultaneous application of Hg and Xe lamp (Xe–Hg experiments). In the experiments, intensity of Hg-radiation decreased at constant Xe-radiation. Shown are isotope data from three series of Xe–Hg experiments performed at pSO_2 = 1013 mbar (black crosses), pSO_2 = 170 mbar (gray crosses), and pSO_2 = 70 mbar (black asterisks). Isotope data from experiments with Hg lamp (black triangles) and Xe lamp (gray triangles) are shown for comparison. Figs. 3c and 3d show magnified data from Xe–Hg experiments performed at pSO_2 = 70 mbar and following parameters: 10% Hg-radiation (number *1*), 5% Hg-radiation (number *2*), and 2% Hg-radiation (number *3*). Dashed line shows sulfur isotope fractionation during SO_2 photolysis using two light sources (Xe and Hg lamps). Solid line shows Archean trends.

experiments at $pSO_2 \approx 70$ mbar (point "3"). Based on the behavior of MIF effects in UP-213–Hg and Xe–Hg experiments, it is reasonable to suggest that the values of $\Delta^{33}S/\delta^{34}S$ and $\Delta^{36}S/\Delta^{33}S$ will vary along corresponding straight lines with a change of the radiation intensity of ArF excimer laser. In the $\delta^{34}S$–$\Delta^{33}S$ diagram (Fig. 5a), a straight line has an intersection with Archean trend in points $\delta^{34}S$ = 43‰ and $\Delta^{33}S$ = 43‰. Hence, in the diagram $\Delta^{33}S$–$\Delta^{36}S$ (Fig. 5b), the value $\Delta^{33}S$ = 43‰ will correspond to $\Delta^{36}S$ = –35‰, which lies in the straight line, near the Archean region. Thus, Archean characteristics can be reproduced for

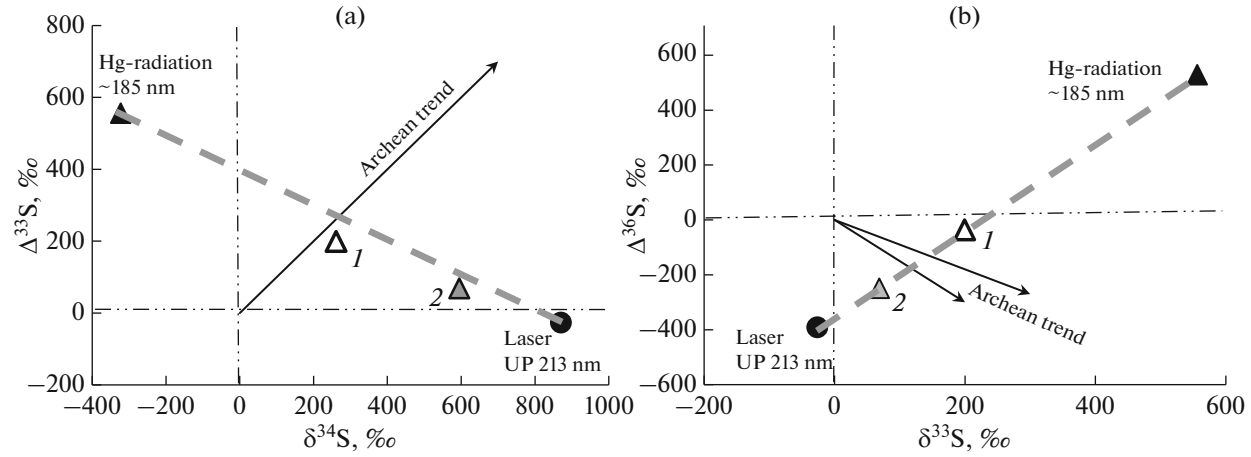

Fig. 4. Relations between $\Delta^{33}S$ and $\delta^{34}S$ (a) and between $\Delta^{33}S$ and $\Delta^{36}S$ (b) for elemental sulfur (product of SO_2 photolysis) from experiments with application of laser system UP-213 (black circles) and UP-213–Hg experiments (triangles *1* and *2*). Dashed line shows sulfur isotope fractionation in UP-213–Hg experiments at change of intensity of Hg-radiation and stable UP-213 radiation.

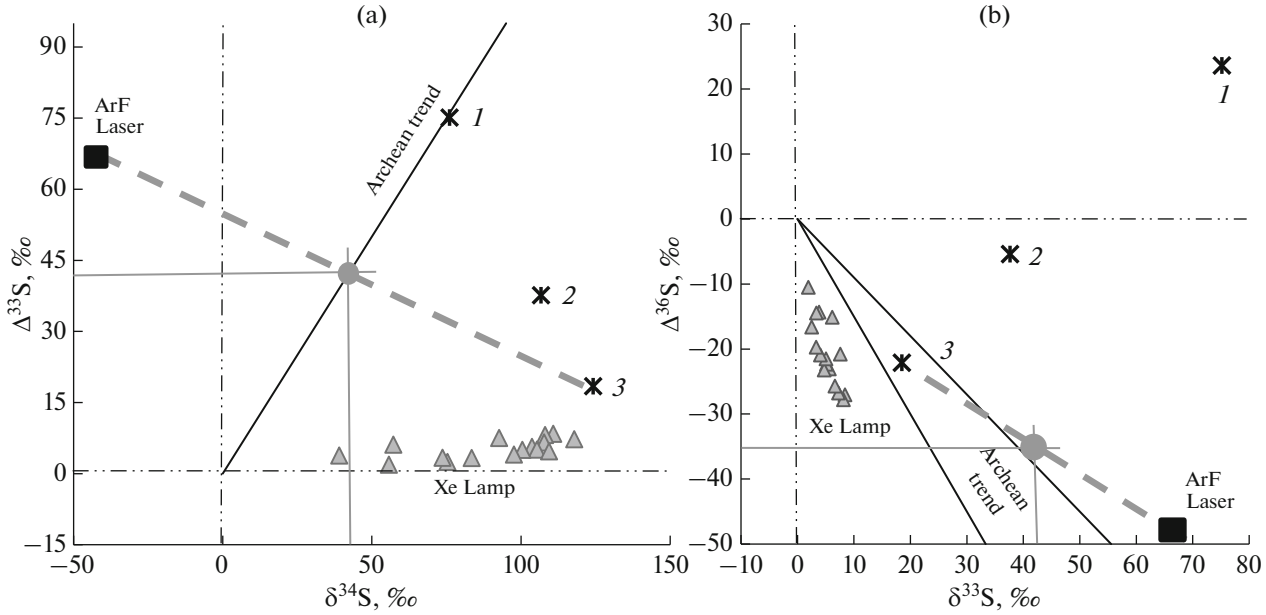

Fig. 5. Isotope data on elemental sulfur obtained in our Xe–Hg experiments (asterisks), together with isotope data obtained in photochemical experiments (Farquhar et al., 2001) with ArF excimer laser $\lambda = 193$ nm (black boxes). Numbers *1*, *2*, and *3* are data the same as in Fig. 3. Dashed line shows predicted sulfur isotope fractionation during SO_2 photolysis using three light sources (Xe and Hg lamps together with ArF excimer laser). Lines of fractionation and Archean trend are intersected at $\Delta^{33}S = 43‰$ (Fig. 5a). Corresponding relations between $\Delta^{33}S$ and $\Delta^{36}S$ (Fig. 5b) lies near the Archean region.

both ratios ($\Delta^{33}S/\delta^{34}S$ and $\Delta^{36}S/\Delta^{33}S$) using shortwave photochemical SO_2 reactions.

Obtained agreement could be occasional, because ignores the influence of other wavelengths at $\lambda < 200$ nm. Nevertheless, the possibility to reproduce the Archean ratios $\Delta^{33}S/\delta^{34}S$ and $\Delta^{36}S/\Delta^{33}S$ within UV range including $\lambda < 200$ nm was shown experimentally, which seemed to be difficult to reproduce in experiments at $\lambda \geq 200$ nm at different conditions (Masterson et al., 2011; Whitehill and Ono, 2012; Ono et al., 2013). These data suggest that the radiation with wavelengths $\lambda < 200$ nm is an essential condition for the production of isotope anomalies in the Archean atmosphere. Given the fact that the dependence of photochemical effects on the shortwave radiation $\lambda < 200$ nm increases with increasing height above the Earth's surface, the MIF effects with Archean $\Delta^{33}S/\delta^{34}S$ and $\Delta^{36}S/\Delta^{33}S$ parameters should be produced during SO_2 photolysis in stratosphere. This conclusion is consistent with assumption (Endo et al., 2019) that SO_2 pho-

tolysis processes generating MIF effects mainly occur in stratosphere. Endo et al. (2019) concluded that Archean MIF effects cannot be produced by SO_2 self-shielding alone, but represent mixed products from both photodissociation and photoexcitation. In our study, the MIF effects comparable with Archean values are mixed products of photochemical reactions initiated by wavelengths $\lambda < 200$ nm. The MIF effects produced during SO_2 photolysis at $\lambda \geq 200$ nm could be related to the mechanism of self-shielding. However, it is impossible to understand MIF effects at $\lambda < 200$ nm from the viewpoint of self-shielding, since the magnitude of isotope anomalies $\Delta^{36}S$ and $\Delta^{33}S$ practically does not depend on the partial SO_2 pressure (or density of SO_2 column), if pSO_2 is slightly lower than one atmosphere (Fig. 2). Therefore, self-shielding alone cannot produce MIF anomalies in Archean rocks.

Considering Xe–Hg experiments as simulation of photochemical state of the early atmosphere, possible conditions required to reproduce Archean $\Delta^{33}S/\delta^{34}S$ and $\Delta^{36}S/\Delta^{33}S$ ratios can be estimated. In our case, such conditions occurred at experimental parameters $pSO_2 \approx 70$ mbar and light flow intensity of Hg lamp ≈2%. Table 2 lists the values of partial SO_2 pressure in experimental chamber for different series and corresponding calculated values of SO_2 contents in an atmospheric air column (SO_2 column density, molecules per cm^2). At $pSO_2 \approx 70$ mbar, the density of SO_2 ccolumn is 1.9×10^{18} molecule/cm^2. This is sufficiently high SO_2 content, which can be observed in the modern atmosphere in the areas of intense volcanic activity. For instance, the air SO_2 concentration during 1991 Pinatubo volcano eruption was >1 ppm, which corresponds to 2×10^{19} molecule/cm^2. The SO_2 content during active volcanic activity could reach hundreds parts per million (ppm) (Kaltenegger and Sasselov, 2010). Based on these data, the experimentally estimated SO_2 content is not unusual for atmospheric conditions and agrees well with inferred relationships between production of MIF effects in the early atmosphere and large SO_2 influx in atmosphere during active volcanic events. Thus, the experimental series with partial SO_2 pressure ~70 mbar can reproduce the Archean atmospheric conditions. The effects of sulfur isotope fractionation under these conditions clearly depend on the spectral composition of radiation. The spectral distribution of Xe and Hg lamps and experimental parameters of radiation indicate that the intensity of solar UV in a shortwave range ($\lambda < 200$) in the Archean should be higher than today. This result is consistent with model concepts that the activity of young sun in the UV region was higher than that of the modern sun (Ribas et al., 2010; Claire et al., 2012). Therefore, the production of sulfur isotope anomalies in the Archean atmosphere was mainly determined by the emission with wavelength <200 nm. This assumption seems to be plausible for SO_2 photolysis in stratosphere, but is hardly possible for troposphere where the UV radiation with $\lambda < 200$ nm is strongly suppressed owing to the absorption by atmospheric carbon dioxide and methane. At the same time, SO_2 is characterized by stronger absorption within a much wider range than CO_2 and CH_4. At sufficiently high SO_2 content in atmosphere, a decrease of UV radiation was likely related to the absorption by SO_2 molecules rather than by CO_2 and CH_4 molecules (Ranjan, 2017). Hence, MIF effects caused by UV radiation <200 nm could occur not only in the stratosphere, but also in troposphere.

It should be noted that the experimentally established dependence of MIF effects on the spectral composition of radiation should not change significantly for SO_2 photolysis in reducing atmosphere. Previous photochemical experiments carried out in the presence of CO_2, H_2O, CH_4 (Farquhar et al., 2001; Whitehill, 2015) did not reveal significant difference between isotope effects produced during photolysis with pure SO_2 (in helium or nitrogen atmosphere) and in the presence of additional gases. Variations in the spectral composition of radiation cause much greater effect on the magnitude and character of sulfur isotope fractionation than the presence or absence of some gas components in atmosphere.

CONCLUSIONS

Series of photochemical experiments were carried out with application of different radiation sources: Xe lamp, low-pressure Hg lamp, and laser system UP-213. It was established that peculiarities of isotope effects $\delta^{34}S$, $\Delta^{33}S$, and $\Delta^{36}S$ in SO_2 photolysis products depend on the spectral characteristics of radiation, intensity of spectral components, and partial SO_2 pressure. Correlations ($\delta^{34}S-\Delta^{33}S$ and $\Delta^{33}S-\Delta^{36}S$) occurred during SO_2 photolysis at $\lambda > 200$ nm sharply differ from those at $\lambda \approx 185$ nm. It was confirmed that the SO_2 photolysis processes in these spectral ranges cannot reproduce MIF effects observed in the Archean rocks. However, as follows from experiments with a simultaneous use of several UV sources in different combination, the observed Archean $\Delta^{33}S/\delta^{34}S$ and $\Delta^{36}S/\Delta^{33}S$ values could be caused by a combination of photochemical processes initiated by radiation in short-wave ($\lambda < 200$ nm) and longer wave ranges. The spectral composition of radiation and the intensity of spectral components are the key parameters determining the variations of $\Delta^{33}S/\delta^{34}S$ and $\Delta^{36}S/\Delta^{33}S$ ratios. A good agreement between Archean and experimentally obtained $\Delta^{33}S/\delta^{34}S$ and $\Delta^{36}S/\Delta^{33}S$ values can be attained only by the involvement of short-wave radiation ($\lambda < 200$ nm) in the photochemical SO_2 dissociation. Hence, the production of sulfur isotope anomalies in Archean atmosphere could be related to

the radiation absorption in a short-wave region ($\lambda <$ 200 nm). In the early atmosphere, these processes could occur both in the stratosphere and troposphere.

FUNDING

The studies were supported by the Russian Foundation for Basic Research (project no. 18-05-00102).

ACKNOWLEDGMENTS

We are grateful to V.B. Polyakov and E.O. Dubinina for their comments, which significantly improved the manuscript.

REFERENCES

M. W. Claire, J. Sheets, M. Cohen, I. Ribas, V. S. Meadows, and D. C. Catling, "The evolution of solar flux from 0.1 nm to 160 μm: quantitative estimates for planetary studies," Astrophys. J. **757**(1) (2012).

M. W. Claire, J. F. Kasting, S. D. Domagal–Goldman, E. E. Stüeken, R. Buick, and V. S. Meadows, "Modeling the signature of sulfur mass-independent fractionation produced in the Archean atmosphere," Geochim. Cosmochim. Acta **141**, 365–380 (2014).

S. O. Danielache, C. Eskebjerg, M. S. Johnson, Y. Ueno, and N. Yoshida, "High-precision spectroscopy of ^{32}S, ^{33}S, and ^{34}S sulfur dioxide: ultraviolet absorption cross sections and isotope effects," J. Geophys. Res. Atmos. **113**, 1–14 (2008).

Y. Endo, S. O. Danielache, Y. Ueno, S. Hattori, M.S.Johnson, N.Yoshida, and H. G. Kjaergaard, "Photoabsorption cross-section measurements of ^{32}S, ^{33}S, ^{34}S, and ^{36}S sulfur dioxide from 190 to 220 nm," J. Geophys. Res. Atmos. **120**, 2546–2557 (2015).

Y. Endo, S. O. Danielache, and Y. Ueno, "Total pressure dependence of sulfur mass-independent fractionation by SO_2 photolysis," Geophys. Res. Lett. **46**, 483–491 (2019).

Y. Endo, Y. Ueno, S. Aoyama, and S. O. Danielache, "Sulfur isotope fractionation by broadband UV radiation to optically thin SO_2 under reducing atmosphere," Earth Planet. Sci. Lett. **453**, 9–22 (2016).

J. Farquhar, H. Bao, and M. Thiemens, "Atmospheric influence of Earth's earliest sulfur cycle," Science **289**, 756–759 (2000).

J. Farquhar, J. Savarino, S. Airieau, and M. H. Thiemens, "Observation of wavelength-sensitive mass–independent sulfur isotope effects during SO_2 photolysis: implications for the early atmosphere," **106**, 32829–32839 (2001).

A. V. Ignatiev, T. A. Velivetskaya, S. Y. Budnitskiy, V. V. Yakovenko, S. V. Vysotskiy, and V. I. Levitskii, "Precision analysis of multisulfur isotopes in sulfides by femtosecond laser ablation GC-IRMS at high spatial resolution," Chem. Geol. **493**, 316–326 (2018).

A. V. Ignatiev, T. A. Velivetskaya, and V. V. Yakovenko, "Effect of mass-independent isotope fractionation of sulfur ($\Delta^{33}S$ and $\Delta^{36}S$) during SO_2 photolysis in experiments with a broadband light source," Geochem. Int. **57** (7), 751–760 (2019).

L. Kaltenegger and D. Sasselov, "Detecting planetary geochemical cycles on exoplanets: Atmospheric signatures and the case of SO_2," Astrophys. J. **708** (2), 1162–1167 (2010).

J. R. Lyons, "Mass–independent fractionation of sulfur isotopes by isotope–selective photodissociation of SO_2," Geophys. Res. Lett. **34**, 1–5 (2007).

J. R. Lyons, "Atmospherically-derived mass-independent sulfur isotope signatures, and incorporation into sediments," Chem. Geol. **267**, 164–174 (2009).

S. L. Manatt and A. L. Lane, "A compilation of the absorption cross sections of SO_2 from 106 to 403 nm," J. Quant. Spectrosc. Radiat. Transfer. **50**, 267–276 (1993).

A. L. Masterson, J. Farquhar, and B. A. Wing, "Sulfur mass-independent fractionation patterns in the broadband UV photolysis of sulfur dioxide: pressure and third body effects," Earth Planet. Sci. Lett. **306**, 253–260 (2011).

Ono, S. "Photochemistry of sulfur dioxide and the origin of mass–independent isotope fractionation in Earth's atmosphere," Annu. Rev. Earth Planet. Sci. **45**, 301–329 (2017).

S. Ono, J. L. Eigenbrode, A. A. Pavlov, P. Kharecha, D. Rumble, J. F. Kasting, and K. H. Freeman, "New insights into Archean sulfur cycle from mass-independent sulfur isotope records from the Hamersley Basin, Australia," Earth Planet. Sci. Lett. **213**, 15–30 (2003).

S. Ono, A. R. Whitehill, and J. R. Lyons, "Contribution of isotopologue self-shielding to sulfur mass-independent fractionation during sulfur dioxide photolysis," J. Geophys. Res. Atmos. **118**, 2444–2454 (2013).

A. A. Pavlov and J. F. Kasting, "Mass–independent fractionation of sulfur isotopes in archean sediments: Strong evidence for an anoxic archean atmosphere," Astrobiology. **2**, 27–41 (2002).

S. Ranjan, The UV Environment for Prebiotic Chemistry: Connecting Origin-of-Life Scenarios to Planetary Environments, *Doctoral Dissertation* (Harvard University, Graduate School of Arts & Sciences, 2017). http://nrs.harvard.edu/urn–3:HUL.InstRepos:41142052

I. Ribas, G. F. Porto De Mello, L. D. Ferreira, E. Hébrard, F. Selsis, S. Catalán A., Garcés, J. D. Do Nascimento, and J. R. De Medeiros, "Evolution of the solar activity over time and effects on planetary atmospheres. II. κ1 Ceti, an analog of the sun when life arose on earth," Astrophys. J. **714**, 384–395 (2010).

T. A. Velivetskaya, A. V. Ignatiev, V. V. Yakovenko, and S. V. Vysotskiy, "An improved femtosecond laser-ablation fluorination method for measurements of sulfur isotopic anomalies ($\Delta^{33}S$ and $\Delta^{36}S$) in sulfides with high precision," Rapid Commun. Mass Spectrom. **33**, 1722–1729 (2019).

N. V. Vyazovetskaya and Yu. V. Vyazovetsky, "Obtaining mercury isotopes by photochemical method," Perspectiv. Mater. **514**, 93–99 (2013).

A. R. Whitehill, Mass-Independent Sulfur Isotope Fractionation during Photochemistry of Sulfur Dioxide, *Doctoral Dissertation*, (Massachusetts Institute of Technology, 2015)

A. R. Whitehill and S. Ono, "Excitation band dependence of sulfur isotope mass-independent fractionation during photochemistry of sulfur dioxide using broadband light sources," Geochim. Cosmochim. Acta **94**, 238–253 (2012).

Translated by M. Bogina